LA-UR-12-24093
Approved for public release; distribution is unlimited.

Title: Application of Stereo Vision to the Reconnection Scaling Experiment

Author(s): Klarenbeek, Johnny
Sears, Jason A.
Gao, Kevin W.
Intrator, Thomas P.
Weber, Thomas

Intended for: Report for PPPL NUF Summer Program

Application of Stereo Vision to the Reconnection Scaling Experiment

J. Klarenbeek[1,2], J. A. Sears[1], K. W. Gao[1], T. P. Intrator[1], T. E. Weber[1]

[1]*Los Alamos National Lab, Los Alamos, New Mexico, 87544*
[2]*University of Central Florida, Orlando, Florida, 32816*

The measurement and simulation of the three-dimensional structure of magnetic reconnection in astrophysical and lab plasmas is a challenging problem. At Los Alamos National Laboratory we use the Reconnection Scaling Experiment (RSX) to model 3D magnetohydrodynamic (MHD) relaxation of plasma filled tubes. These magnetic flux tubes are called flux ropes. In RSX, the 3D structure of the flux ropes is explored with insertable probes. Stereo triangulation can be used to compute the 3D position of a probe from point correspondences in images from two calibrated cameras. While common applications of stereo triangulation include 3D scene reconstruction and robotics navigation, we will investigate the novel application of stereo triangulation in plasma physics to aid reconstruction of 3D data for RSX plasmas. Several challenges will be explored and addressed, such as minimizing 3D reconstruction errors in stereo camera systems and dealing with point correspondence problems.

I. Introduction

Magnetic reconnection is a fundamental process in plasma physics in which local breaking of magnetic field lines results in a restructuring of the magnetic field and a release of stored magnetic energy in the form of plasma flow [1]. It is studied widely in astrophysical and laboratory plasmas, such as solar flares [2] and magnetic fusion plasmas, where it can degrade particle and energy confinement [3].

In the Reconnection Scaling Experiment (RSX), 3D magnetic reconnection is studied in parallel plasma current channels (flux ropes) which mutually attract. RSX uses multiple probe positioners that facilitate the collection of 3D data by enabling precise movement of the probes in three dimensions [5].

Stereo triangulation can be used to compute the 3D position of a point from its projection in two images by computing the intersection of rays originating from the camera lens center and passing through the corresponding image points [6]. This requires knowledge of the intrinsic parameters for both cameras, which describe the direction of a ray projecting out of a pixel on the image. In addition, the extrinsic parameters of the cameras are also required, which describe one camera's rotation and translation with respect to the other.

Various camera calibration procedures exist to determine the intrinsic and extrinsic parameters in a stereo camera configuration [7]. It is important to choose the most accurate method available as an improper calibration can be a major source of error in all measurements. The other major source of error is the error in identifying exact point correspondences in both images in a stereo system, which results in the projected rays not intersecting in 3D. The points must be displaced in such a way that this reprojection error is minimized. There are several solutions available that address this problem [8,9].

In some instances it is possible for the insertable probes to be obscured in one of the camera views. This means we cannot implement a fully automatic solution that will determine the position of the probes without any user interaction. We will address these issues and implement a solution that will be able to compute the 3D position of the probes when only visible in one camera view.

II. Technical Description

To provide a framework for the stereo triangulation process we will first introduce the simple linear pinhole camera model. **Figure 1** depicts a simple linear pinhole camera model, which maps a point from 3D space to the image plane. In Euclidian space $\mathbb{R}^3$ the mapping of beam direction $M' = [X', Y', Z']^T$ to image coordinates

$\widetilde{m} = [u, v, 1]^T$ is achieved by first projecting it onto the plane $Z' = 1$ and multiplying the normalized image coordinates by the intrinsic camera matrix as described in equations **(1.1)** and **(1.2)** [10].

$$\widetilde{m} = \begin{bmatrix} u \\ v \\ 1 \end{bmatrix} = K \begin{bmatrix} x \\ y \\ 1 \end{bmatrix} = K \begin{bmatrix} X'/Z' \\ Y'/Z' \\ 1 \end{bmatrix} \quad (1.1)$$

$$K = \begin{bmatrix} f & 0 & u_0 \\ 0 & f & v_0 \\ 0 & 0 & 1 \end{bmatrix} \quad (1.2)$$

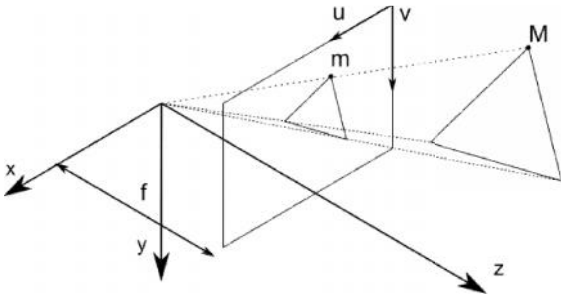

Figure 1: Projective mapping of 3D object onto image plane

The intrinsic camera matrix consists of the focal distance f (scale factors) and the principal point u_0, v_0 (the intersection of the optical axis with the image plane). In order to be able to model a real camera as a pinhole camera, the geometric lens distortion must be computed and reversed. Equations **(2.1) – (2.3)** describe the mapping of normalized points to distorted image coordinates using a model that takes into account radial and tangential lens distortion [11]. K1, k2, k3, and k4 are the distortion coefficients calculated in the camera calibration step. The normalized points are related to the beam direction M' by equation **(1.1)**.

$$\begin{cases} u = u_o + fx' \\ v = v_0 + fy' \end{cases} \quad (2.1)$$

$$\begin{cases} x' = x(1 + k_1 r^2 + k_2 r^4) + k_3(3x^2 + y^2) + 2k_4 xy \\ y' = y(1 + k_1 r^2 + k_2 r^4) + 2k_3 xy + k_4(x^2 + 3y^2) \end{cases} \quad (2.2)$$

$$r = \sqrt{x^2 + y^2} \quad (2.3)$$

Figure 2 depicts a stereo camera model showing the paths of beams of light passing from 3D point P through the center of projections onto the image planes.

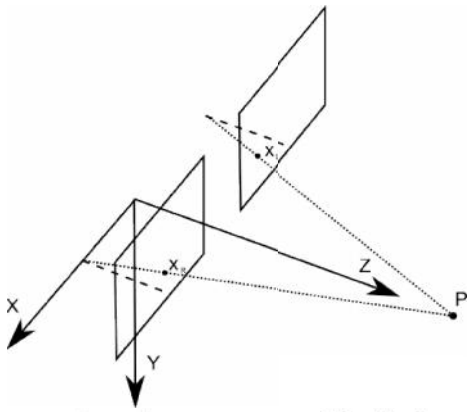

Figure 2: Perspective projection of point P onto left and right camera planes

Let $\overline{X_R} = [X_R\ Y_R\ Z_R]$ and $\overline{X_L} = [X_L\ Y_L\ Z_L]$ be the coordinates of point P in the right and left camera reference frames. The left camera frame is related to the right camera frame by a translation and a rotation:

$$\overline{X_L} = R\overline{X_R} + T \quad (3.1)$$

The vectors of the perspective projections of point P onto the camera planes are $\overline{x_R} = \frac{\overline{X_R}}{Z_R} = [x_R\ y_R\ 1]^T$ and $\overline{x_L} = \frac{\overline{X_L}}{Z_L} = [x_L\ y_L\ 1]^T$. Our goal is to solve for Z_R and Z_L and then solve for the remaining coordinates. Equation **(3.1)** can be rewritten as:

$$[-R\overline{x_R}\ \ \overline{x_L}] \begin{bmatrix} Z_R \\ Z_L \end{bmatrix} = T \quad (3.2)$$

Let $A = [-R\overline{x_R}\ \ \overline{x_L}]$. The least squares solution can be written as:

$$\begin{bmatrix} Z_R \\ Z_L \end{bmatrix} = (A^T A)^{-1} A^T T \quad (3.3)$$

Letting $\overline{\alpha_R} = -R\overline{x_R}$, an explicit solution for equation **(3.3)** may be derived [12]:

$$Z_R = \frac{\|\overline{x_L}\|^2 (\overline{\alpha_R} \cdot T) - (\overline{\alpha_R} \cdot \overline{x_L})(\overline{x_L} \cdot T)}{\|\overline{\alpha_R}\|^2 \|\overline{x_L}\|^2 - (\overline{\alpha_R} \cdot \overline{x_L})^2} \quad (3.4)$$

This solution was implemented in the IDL programming language. The code was largely based off of Bouguet's work on the Matlab Camera Calibration Toolbox [13].

III. Design Considerations

The biggest challenges faced in this project are dealing with situations where a probe is obscured in one camera view and transforming the 3D coordinates from the camera reference frame to the RSX origin coordinate system. **Figure 3** illustrates the two cameras looking into the end of the RSX machine.

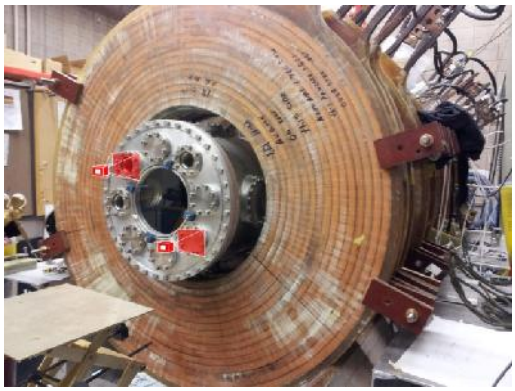

Figure 3: Drawing of camera views looking into the RSX machine

Stereo triangulation cannot be employed in situations where a probe is partially obscured in one of the camera views. To overcome this problem we will measure the Z distance of the probes to a reference point (origin) inside RSX and use stereo triangulation to obtain the distance from this reference point to the cameras. The total distance can then be used to determine the 3D coordinates of the probes. See **figure 4** for a view of the probes from one of the viewport cameras.

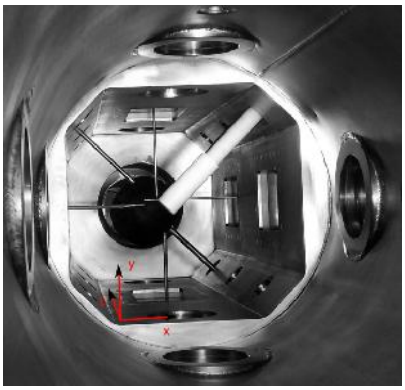

Figure 4: View of probes inside RSX showing how probes can be obstructed by the plasma gun (white cylindrical object)

In order to be able to accurately determine the position of the probes the cameras must be perfectly aligned (perpendicular) to the Z axis in RSX. It is difficult to align the cameras to be perfectly perpendicular to RSX. Therefore, the best solution is to find the rotation of the cameras relative to the RSX origin and transform the 3D coordinates in order to align them with the RSX coordinate system. Once the probe position has been found relative to the cameras a rotational and translational transform can be applied in order to recover the probe position relative to the machine origin.

In an effort to automate part of the probe position measurement process we have implemented a procedure that detects a set of coplanar points on the XY plane in RSX on the set of images collected from the stereo camera setup. **Figure 5** provides an overview of the corner detection process.

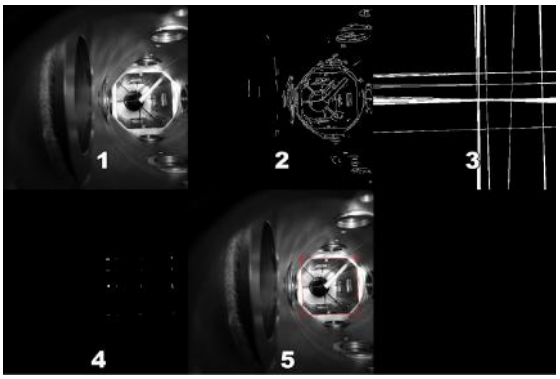

Figure 5: Edge / Point detection process used to identify XY plane of RSX

The four coplanar points on the XY plane of RSX are detected as follows:

1. Canny edge detection is performed. A threshold was chosen that eliminates most unnecessary lines.
2. A Hough transform detects lines and maps them to parameter space, where each line is represented by a (r, θ) coordinate pair.
3. The lines are filtered to reject all lines that are below a certain length and lines that do not lie nearly horizontal or vertical.
4. Points where horizontal lines intersect vertical lines are identified as corner points for the XY plane.

3D coordinates for the coplanar points are obtained through stereo triangulation. A normal is

projected from 3 coplanar points and compared to the normal $(0, 0, 1)$. This allows us to determine the rotation of the plane in two dimensions. After reversing this rotation the third rotation can be easily obtained and reversed. All of the procedures discussed so far form the foundation that enables determination of the 3D position of all probes with respect to the origin of RSX given the Z distance of the probes to this point.

IV. Experiment

In order to test the feasibility of a stereo camera setup on the RSX machine an experiment was set up to simulate the distances involved in triangulation of the probes in the vacuum chamber.

A single camera (Sony IMX105PQ CMOS sensor) was mounted on a rail mount on an optical table in order to be able to precisely control the distance between cameras in our pseudo stereo camera setup. Images were taken at a resolution of 2048x1536 pixels. The distance between cameras was chosen to be 30mm as this roughly corresponds to the distance between viewports on the end of the RSX chamber. The camera was calibrated using DLR CalDe and CalLab [14].

Stereo triangulation was performed on a checkerboard target with squares of known size (20mm) at distances of 60cm, 120cm, and 180cm. The distance of 180cm was chosen because this roughly corresponds to the distance of the insertable probes in the machine to the viewport.

All 130 points on the checkerboard pattern were detected on the test images and after stereo triangulation the lengths of all sides of the squares on the checkerboard pattern were measured in 3D. These were compared to the known reference size of 20mm to obtain the error measurement. 237 measurements were obtained for each stereo pair of images processed. **Figure 6** shows a pair of test images taken at a distance of 60cm from the target.

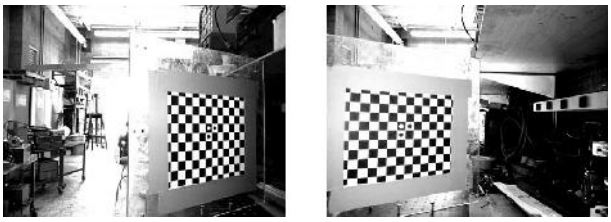

Figure 6: Stereo image pair from experiment

Figure 7 depicts histograms of error distributions for each distance from the target. Units of measurement are in mm. As expected the error generally increases as distance measured increases.

The wide spread in error distribution is most likely due to errors in detecting point correspondences in stereo image pairs. The checkerboard pattern corners were detected using DLR CalDe.

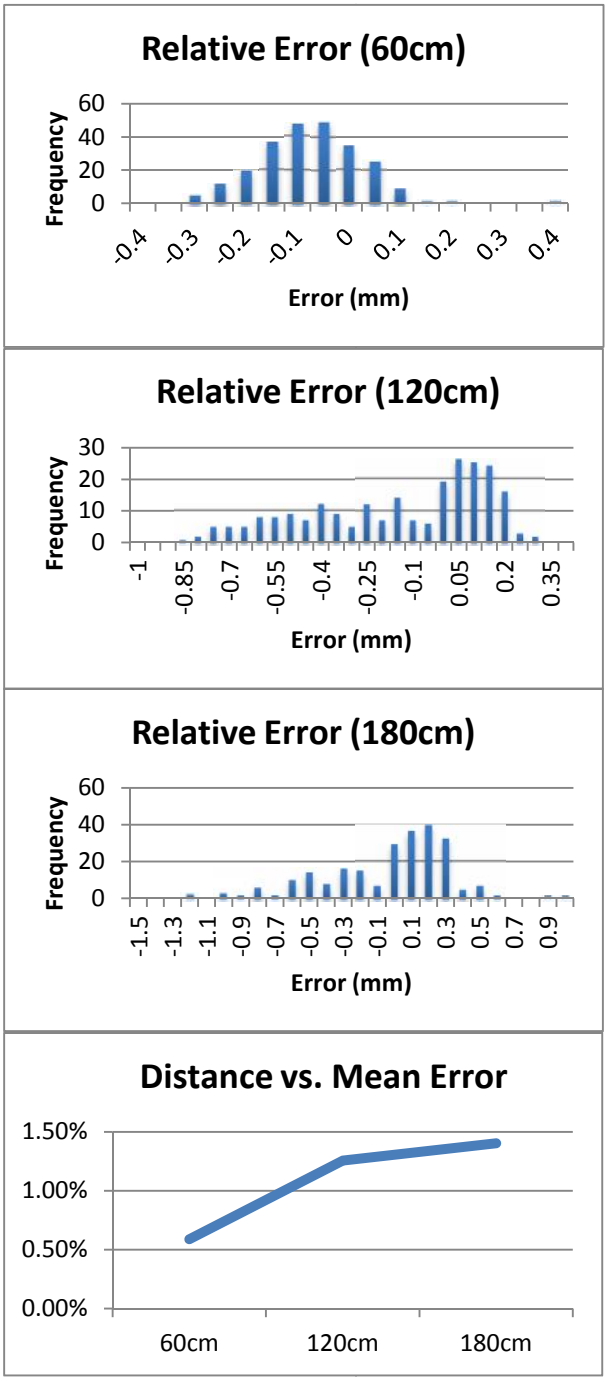

Figure 7a-d: Histograms of error and mean error percentage vs distance

V. Conclusion

Our results have shown that stereo triangulation is a very accurate technique to determine the position of multiple probes inside a vacuum chamber. The largest mean error in the checkerboard pattern reprojection was 1.4% at a distance of 180cm. This is an acceptable level of error that will be comparable in real probe measurements since the probes will perform data measurements in a sweep across the chamber resulting in a set of position points similar to the shape of the checkerboard pattern. The largest source of error that will be encountered in future work will be errors in measurement of the Z distance of the probes to the RSX origin as well as errors in selecting probe points in camera images.

In future work we will implement our stereo camera setup on the viewport at one end of the RSX machine and utilize the setup to collect 3 dimensional data from the experiment.

While we have implemented all of the code necessary to detect the 3D position of any probe in the RSX vacuum chamber, it is challenging to find a set of inexpensive high resolution cameras that have a common lens mount such as the C-mount or CS-mount. Obtaining a highly accurate measurement of the probe positions requires a high resolution camera that can be modified to have a small field of view so that no pixels are wasted on imaging the part of the chamber that won't be used in the positioning of the probes.

A practical addition to this project would be to automate the detection of probe points just like the already existing detection of plane corners so that the only user input required is the Z distances of the probes to the RSX origin point. A major challenge involved in realizing this feature is developing a robust algorithm that can accurately detect the same point on the probe in each image. In addition, stereo triangulation could be performed automatically for probes that are visible in both camera image planes to reduce the amount of user input required.

VI. Acknowledgements

This work was supported by DOE Office of Fusion Energy Sciences under LANS contract DEAC52-06NA25369, NASA Geospace NNHIOA044I, Basic. Also supported by NASA, Los Alamos National Lab, Princeton Plasma Physics Laboratory, and the National Undergraduate Fellowship Program.

VII. References

[1]Eric Priest, Terry Forbes, Magnetic Reconnection, Cambridge University Press 2000, ISBN 0-521-48179-1,
[2]Magnetic Reconnection in Solar and Astrophysical Plasmas K. Shibata Kwasan Observatory, Kyoto University, Yamashina, Kyoto 607-8471, Japan
[3]MHD INSTABILITIES IN TOKAMAKS H.J. de Blank FOM-Institute for Plasma Physics Rijnhuizen
[4]Experimental onset threshold and magnetic pressure pile-up for 3D reconnection T. P. Intrator *, X. Sun, G. Lapenta, L. Dorfand I. Furno
[5]A three dimensional probe positioner, T. Intrator, X. Sun, L. Dorf, I. Furno, and G. Lapenta
[6]Hartley, R., Zisserman, A.: Multiple View Geometry in Computer Vision. 2nd ed., Cambridge University Press, Cambridge (2004)
[7]Semi-automatic Camera Calibration Using Coplanar Control Points, Rune H. Bakken, Bjørn G. Eilertsen, Gustavo U. Matus, Jan H. Nilsen, Sør-Trøndelag University College
[8]Hartley, R.I., Sturm, P.: Triangulation, Comput. Vision Image Understand. 68(2),146–157 (1997)
[9]Kanatani, K.: Statistical Optimization for Geometric Computation: Theory and Practice. Elsevier, Amsterdam (1996); reprinted, Dover, York (2005)
[10]GEOMETRIC STEREO CAMERA CALIBRATION WITH DIFFRACTIVE OPTICAL ELEMENTS, Denis Grießbach, Martin Bauer, Martin Scheele, Andreas Hermerschmidt, Sven Kruger†
[11]A Technique for Binocular Stereo Vision System Calibration by the Nonlinear Optimization and Calibration Points with Accurate Coordinates, H Chen, D Ye, R S Che and G Chen
[12]P. Schröder, J. Y. Bouguet and M. Gavriliu, Stereo Triangulation in Matlab. http://www.multires.caltech.edu/teaching/courses/3DP/ftp/98/hw/1/triangulation.ps, 2004
[13]J.-Y. Bouguet, Camera Calibration Toolbox, http://www.vision.caltech.edu/bouguetj/calib doc/, 2004.
[14]K. Strobl, W. Sepp, S. Fuchs, C. Paredes, and K. Arbter. DLR CalDe and DLR CalLab. Institute of Robotics and Mechatronics, German Aerospace Center (DLR), Oberpfa enhofen, Germany. Available at http://www.robotic.dlr.de/callab/. 2, 4, 6, 10